Effects of XX-catalysts on quantum annealing spectra with perturbative crossings

Natasha Feinstein* and Louis Fry-Bouriaux London Centre for Nanotechnology, University College London, WC1H 0AH London, UK

Sougato Bose

Department of Physics and Astronomy, University College London, London WC1E 6BT, UK and Department of Electronic & Electrical Engineering, University College London, WC1E 7JE London, UK

P. A. Warburton

London Centre for Nanotechnology, University College London, WC1H 0AH London, UK and
Department of Electronic & Electrical Engineering,
University College London, WC1E 7JE London, UK
(Dated: March 15, 2022)

The efficiency of Adiabatic Quantum Annealing is limited by the scaling with system size of the minimum gap that appears between the ground and first excited state in the annealing energy spectrum. In general the algorithm is unable to find the solution to an optimisation problem in polynomial time due to the presence of avoided level crossings at which the gap size closes exponentially with system size. One promising avenue being explored to produce more favourable gap scaling is the introduction of non-stoquastic XX-couplings in the form of a catalyst - of particular interest are catalysts which utilise accessible information about the optimisation problem in their construction. Here we show extreme sensitivity of the effect of an XX-catalyst to subtle changes in the encoding of the optimisation problem. We observe that catalysts designed to enhance the minimum gap at an avoided level crossing can, under certain conditions, result in closing gaps in the spectrum. To understand the origin of these closing gaps, we study how the evolution of the ground state vector is altered by the presence of the catalyst. We find that the negative components of the ground state vector are key to understanding the response of the gap spectrum. In particular the closing gaps correspond to changes in which vector components become negative over the course of the evolution. We also consider how and when these closing gaps could be utilised in diabatic quantum annealing protocols - a promising alternative to adiabatic quantum annealing in which transitions to higher energy levels are exploited to reduce the run time of the algorithm.

I. INTRODUCTION

Quantum annealing (QA) is a continuous time quantum algorithm proposed as a means of solving NP combinatorial optimisation problems faster than can be achieved classically [1–3]. It proceeds by initialising a quantum system in the ground state of a simple Hamiltonian, referred to as the driver and conventionally chosen to be a local transverse field, and evolving to a Hamiltonian whose ground state encodes the optimal solution of the problem to be solved. If the evolution proceeds adiabatically, the ground state of the final Hamiltonian is obtained with high probability at the end of the anneal. A suitable evolution rate is determined by the adiabatic theorem [4]. In its simplest form, this states that the total evolution duration must scale inversely with the square of the minimum energy gap between the ground and first excited states in the energy spectrum of the total Hamiltonian. Whether or not QA is capable of solving a problem efficiently thus depends on how this minimum gap scales with the problem size.

Early results that focused on randomly generated instances of the exact-cover problem for small system sizes suggested that the minimum energy gap scaling may be polynomial [5], which would allow QA to find the solution efficiently. However subsequent studies have suggested that we can generally expect exponentially closing gaps in the annealing spectrum resulting from the presence of first order phase transitions [6–10]. A particular problem which has been highlighted is the potential for so called perturbative crossings to form between the low energy eigenstates of the problem Hamiltonian towards the end of the anneal [11, 12]. The corresponding energy gap has been found to be exponentially small with the Hamming distance between the eigenstates, which can generally be expected to grow with the system size [11]. Additionally, it was argued in [12] that the probability of such a crossing occurring would grow exponentially with the number of states that had energy comparable to that of the ground state, suggesting that the likelihood of not encountering such a transition vanishes with increasing problem size.

These results suggest that quantum annealing in its standard formulation, in which the driver and the problem Hamiltonian are interpolated monotonically and homogeneously, is unlikely to lead to performance advantages over classical algorithms. As such, new avenues are being explored for circumventing the computation time scaling problem associated with adiabatic evolution by

^{*} ucapnjs@ucl.ac.uk

changing the path the anneal takes from the driver to the problem Hamiltonian. These new methods typically focus on the inhomogeneous driving of the transverse field [13–19] or the introduction of an additional term to the Hamiltonian referred to as a catalyst [9, 16, 20–27]. In general, the goal is to enhance the size of the minimum gap in the annealing spectrum [9, 13–16, 18, 20, 22– 24, 27]. However, a faster time to solution can also be obtained by manipulating the spectrum such that a diabatic anneal is possible [17, 22, 25]. In this case the goal is to produce a path through the annealing energy spectrum that exploits transitions to higher energy states such that the system subsequently returns to the ground state. When this can be achieved, the small energy gaps at which these transitions happen no longer present bottlenecks to the algorithm, and if all other gaps in the spectrum close no faster than polynomially with system size, QA will be able to efficiently find the ground state of the problem Hamiltonian. This exploitation of transitions has been shown to result in exponential speedup for the glued trees problem whose structure results in a symmetric annealing spectrum that is naturally amenable to diabatic QA [28].

The effects of different general strategies for manipulating the spectrum have been studied for various systems. For instance, staggering the times at which the transverse field starts decreasing has been found to reduce the residual energy at the end of the anneal for a weakly disordered quantum spin chain [19] and remove the first order phase transition present for the p-spin model [15]. Additionally, non-stoquastic XX-catalysts have been shown to reduce the first order phase transition to second order for both the p-spin [9, 23] and the Hopfield model [21]. However the same strategies do not always lead to the same results in different settings. For instance, it was found that for the frustrated Ising ladder, neither stoquastic nor non-stoquastic XXinteractions were able to remove the first order phase transition [29]. For a mean field version of the weakstrong cluster problem it was found that whether stoquastic XX-couplings or non-stoquastic ones removed the phase transition depended on where the couplings were applied [16]. Additionally, it was shown in [30] that nonstoquastic Hamiltonians generally have smaller gaps than stoquastic ones, suggesting that the addition of a term that makes the Hamiltonian non-stoquastic could in some cases result in a less favourable gap scaling.

There have also been studies examining strategies that exploit pre-existing or accessible knowledge of the problem structure to alter the annealing path. It was shown in [14] how knowledge of the local optima could be used to adjust the relative strengths of the local X-fields to remove or weaken perturbative crossings. In [31] Choi shows that a similar result can be achieved using XX-couplings. A more recent work [25] shows that by coupling local optima to each other, one can replace a single avoided level crossing with a correlated double avoided level crossing - thus facilitating a diabatic anneal. Strate-

gies such as these are particularly appealing since it may be possible to access the required prior information in polynomial time by running the anneal quickly and/or using classical algorithms. For this strategy to be viable, it is important to study how and why different changes to the annealing path affect the gap spectrum.

In this paper we examine the effect of a targeted XXcatalyst designed to enhance the minimum gap size at a perturbative crossing. This catalyst is inspired by ideas introduced in [24, 25, 31] where the effect a catalyst has is tied to the couplings it induces between problem states. Using the maximum weighted independent set (MWIS) problem to construct our annealing instances, we show that the effect of this catalyst is strongly dependent on arbitrary small changes to the parameters of the problem Hamiltonian which alter the properties of the perturbative crossing that forms in the original spectrum. In particular we observe that, while under certain conditions we are able to replicate the gap enhancement seen for similar catalysts, this catalyst can also result in closing gaps in the annealing spectrum. More specifically, we observe that as we increase the strength of the catalyst, we first observe a closing of the gap at the perturbative crossing followed by the formation of an additional gap minimum earlier in the anneal.

We begin by describing the structure of our annealing Hamiltonian in section 1 before going on, in section IIB, to motivate and explain the structure of our MWIS problems. This we supplement with numerical results that show we are able to produce the desired annealing spectra - that is, we are able to produce a perturbative crossing and tune the severity of the associated gap scaling. With the problem setting established we then, in section III, move on to examining the effects of introducing targeted non-stoquastic XX-catalysts. We describe our choice of catalyst and show, in section III A, that for parameter settings which result in a softer perturbative crossing, that the catalyst is able to significantly reduce the gap closing with system size. We then, in section IIIB, apply the same catalysts to the perturbative crossing with harsher gap scaling and, in this setting, we observe the aforementioned closing gaps. In order to shed some light on the source of these closing gaps, as well as why the effect of the catalyst differs in these two settings, we examine how the evolution of the ground state vector is affected by the increase in the presence of the catalyst.

II. PROBLEM SETTING

We are interested in examining the effects of XX-couplings on perturbative crossings - a type of avoided level crossing (AC) between problem states that are close in energy that can form towards the end of the anneal. In particular, we are looking to compare the effects of the same XX-coupling on perturbative crossings with different associated gap scaling. To this effect we construct a scalable instance of the MWIS problem that allows us to

easily adjust key properties of the problem Hamiltonian that are responsible for the formation of such crossings. The MWIS problem is a natural choice due to the free parameters present in the encoding of the problem into an Ising Hamiltonian as well as the ease with which we can change the energies of the states which are one bit flip apart from each other - the importance of this will become clear in section IIB. The MWIS problem is also NP-complete meaning that any other problem in NP can be mapped on to it.

We begin this section by describing our total annealing Hamiltonian as well as the catalysts that we will be using. We then, in section II B, go on to explain the conditions under which perturbative crossings form - motivating the construction of our MWIS graph. We demonstrate with numerical examples that this setting does indeed produce the expected ACs and that we are able to adjust their properties. We stress that section II B focuses purely on the annealing spectrum prior to the introduction of a catalyst.

A. Hamiltonian

Our annealing Hamiltonian takes the form

$$H(s) = (1 - s)H_d + s(1 - s)H_c + sH_p, \tag{1}$$

where H_d , H_c and H_p are independent of s and denote the driver, catalyst and problem Hamiltonians respectively. The dimensionless annealing parameter, s, is varied from 0 to 1 over the course of the anneal such that H(s) evolves from $H(0) = H_d$ to $H(1) = H_p$. We consider the anneal in a static setting and so it is not necessary to specify how s is varied with time except to say that it increases monotonically such that the same part of the annealing spectrum is not crossed more than once. We refer to the eigenstates of the total Hamiltonian as the *instantaneous* eigenstates and denote them and their corresponding energies as

$$H(s) |E_a(s)\rangle = E_a(s) |E_a(s)\rangle.$$
 (2)

The states are labelled starting from a=0 in order of increasing energy. Similarly we denote the *problem* eigenstates and their energies as

$$H_p |E_a\rangle = E_a |E_a\rangle. \tag{3}$$

Since the problem Hamiltonian is diagonal in the computational basis, the set of problem states $\{|E_a\rangle\}$ is simply the computational basis with the states labelled by energy.

Our choice of driver is the conventional homogeneous local X-field,

$$H_d = -\sum_{i=1}^n \sigma_i^x,\tag{4}$$

where n is the total number of qubits and σ_x^i denotes the Pauli-X operator on the *i*th qubit. Its ground state is the equal superposition over all computational basis states. The catalysts used in this work contain a single XX-coupling between two qubits and can thus be written,

$$H_c = J_{xx} \sigma_i^x \sigma_i^x. \tag{5}$$

where J_{xx} is always chosen to be positive such the total Hamiltonian is non-stoquastic for $s \neq 0, 1$. Its magnitude can be tuned to adjust the strength of the catalyst relative to H_d and H_p . We note that here we are using the term non-stoquastic simply to describe a Hamiltonian with positive as well as negative off diagonal elements. This does not necessarily imply that these Hamiltonians would be hard to simulate classically (i.e: with quantum Monte Carlo encountering the sign problem [32]) or that there is no basis in which H(s) has all real, non-positive off diagonal elements. We make no assumptions regarding the relationship between non-stoquasticity and computational complexity.

We now go on to describe the motivation for and construction of our problem Hamiltonians.

B. Problem Graph

Our problem instances are constructed to produce annealing spectra with perturbative crossings - a well understood bottleneck in QA that can arise when excited states of the problem Hamiltonian have an energy comparable to that of its ground state [11, 12]. Their presence can be understood by perturbatively introducing H_d to H_p and looking at the energy corrections to the problem states. We briefly outline how this works before going on to describe our problem instances - more precise descriptions of how these ACs form can be found in [11, 12, 14].

Writing the perturbed energies as $E_a(\lambda)$, we can say that a crossing occurs between two problem states a and b if $E_b(\lambda) < E_a(\lambda)$ (b > a) for some λ . If this λ is small enough that perturbation theory remains valid, this indicates the formation of an AC towards the end of the instantaneous gap spectrum. Because the driver Hamiltonian couples problem states that are one spin-flip apart, the perturbation to the state $|E_a\rangle$ is dependent on the states that are within unit hamming distance of $|E_a\rangle$ we refer to this set of states as the neighbourhood of $|E_a\rangle$. It can be shown that the lowest energy problem states will experience a reduction in energy as a result of the perturbation so long as the hamming distance between any pair of these states is greater than 1. The rate of this reduction with respect to λ for each state depends on the energy of the states in its neighbourhood, with lower energies resulting in a greater reduction. Thus a crossing can occur between the ground state and some other problem state $|E_a\rangle$ that is close in energy if the neighbourhood around the state $|E_a\rangle$ contains lower energy states than that around the ground state. The value of λ for which the crossing occurs, and thus whether or not an AC

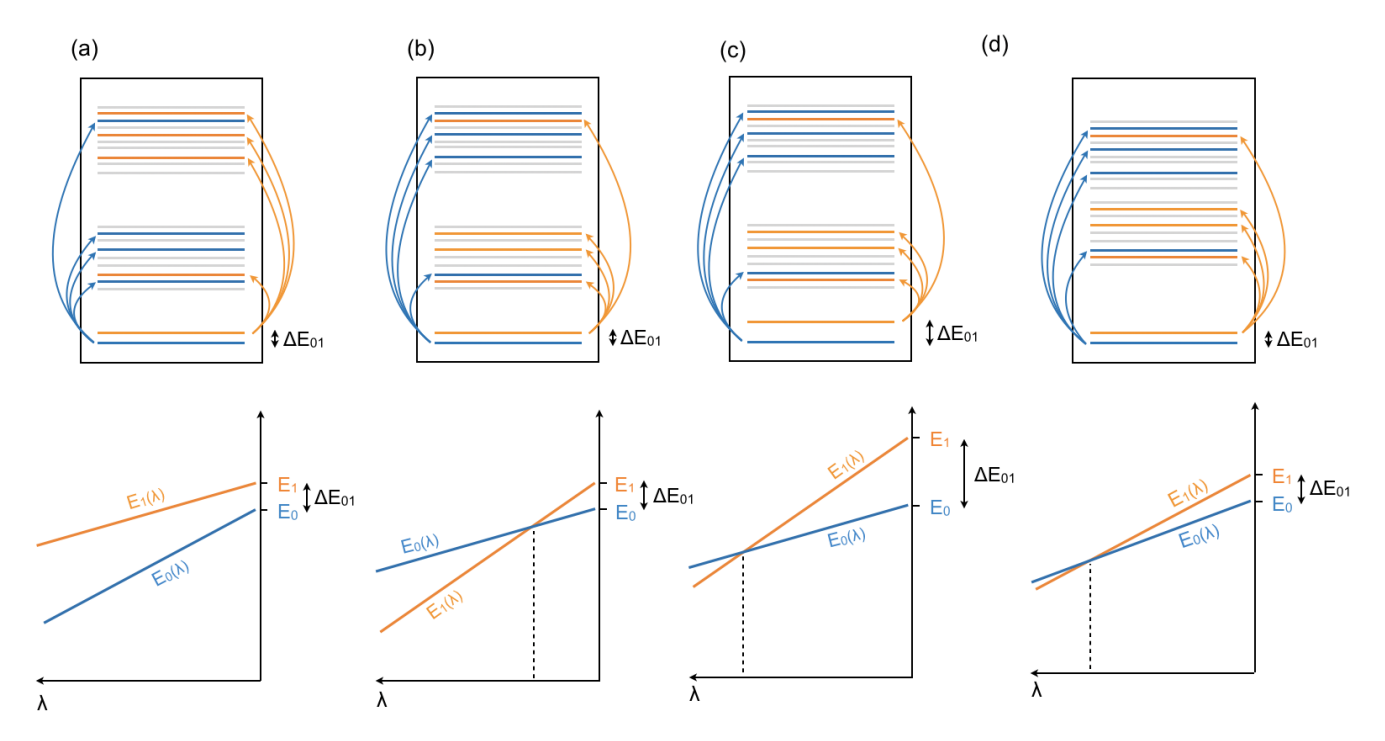


FIG. 1: Top: Cartoon problem energy spectra with the ground and first excited state, as well as their neighbourhoods, highlighted in blue and orange respectively. Bottom: Corresponding cartoons of the perturbed problem energies where the perturbation is the driver Hamiltonian and the perturbative parameter is λ . (a) $|E_0\rangle$ has a lower energy neighbourhood than $|E_1\rangle$ such that no perturbative crossing forms. (b) $|E_1\rangle$ has a lower energy neighbourhood than $|E_0\rangle$ such that a perturbative crossing does form. (c) Similar setting to (b) but with a larger ΔE_{01} such that the crossing happens at larger λ . (d) Similar setting to (b) but where the neighbourhoods are closer in energy, reducing the difference between the gradients of the perturbations, such that the crossing happens at larger λ .

forms, will depend on the difference in energy between the two unperturbed problem states, $\Delta E_{0a} = E_a - E_0$, and how different in energy the neighbourhoods around them are.

The top row of Fig. 1 shows cartoon problem energy spectra with E_0 and its neighbourhood highlighted in blue and E_1 and its neighbourhood in orange. (For clarity we include arrows showing the driver couplings from $|E_0\rangle$ and $|E_1\rangle$ to their respective neighbourhoods.) Corresponding cartoons illustrating the perturbed energies are shown below with the magnitude of the driver increasing from right to left. Fig. 1(a) depicts a setting where $|E_0\rangle$ has a lower energy neighbourhood than $|E_1\rangle$ such that it receives a greater negative perturbation and no crossing forms. Fig. 1(b) depicts the case where the neighbourhoods are reversed such that $|E_1\rangle$ receives a greater negative perturbation and the perturbed energies cross. Fig. 1(c) shows a similar scenario but with a greater ΔE_{01} such that a higher λ is needed before the energies cross. Finally, in Fig. 1(d) ΔE_{01} is the same as in Fig. 1(a) but the difference between the energies of their neighbourhoods is decreased such that the difference between the gradients of the perturbed energies are smaller. This also increases the value of λ for which the crossing occurs.

In addition to changing the value of λ for which the

crossing occurs, and thus the value of s at which we observe an AC in the annealing spectrum, ΔE_{01} and the neighbourhoods around $|E_0\rangle$ and $|E_1\rangle$ also affect the extent to which the perturbed state vectors $|E_a(\lambda)\rangle$ have evolved away from the problem state vectors $|E_a\rangle$ at the point of the crossing. In the case where the differences between $|E_a(\lambda)\rangle$ and $|E_a\rangle$ are minimal, the instantaneous ground state will go from being predominantly occupied by one problem state to another such that the overlap between the instantaneous ground state before and after the AC is very small. However if the perturbed problem states have become more mixed, then the overlap may be larger. The extent of this overlap affects the size of the gap minimum associated with the AC, with a larger overlap leading to a bigger gap [33].

In order to produce an annealing spectrum with a perturbative crossing we thus require a problem setting where E_0 and E_1 are close in energy and where the neighbourhood around $|E_1\rangle$ contains lower energy states than that around $|E_0\rangle$. Additionally, if we wish to be able adjust the sharpness of the crossing, we need to be able to easily tune ΔE_{01} as well as how different the energies of the neighbourhoods are. To achieve this, we utilise the MWIS problem, which takes as its input an undirected, weighted graph and aims to find the set of ver-

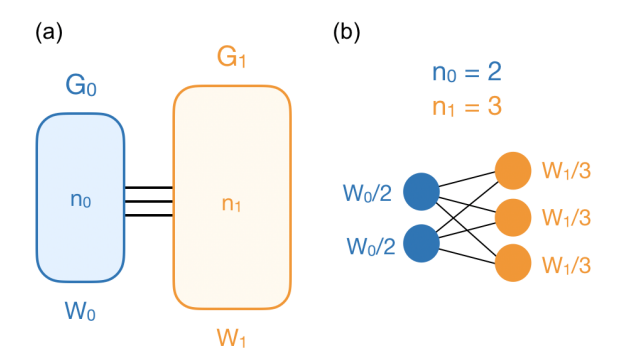


FIG. 2: An illustration of our graph structure, as described in section IIB, is shown in (a). An example with $n_0 = 2$ and $n_1 = 3$ is shown in (b).

tices with the largest weight for which no two vertices are connected by an edge. The problems we construct, as well as the ways we utilise the free parameters in its Ising Hamiltonian encoding, are inspired by the MWIS instances used in [31]. We now describe how the MWIS problem Hamiltonian is constructed before going on to describe our specific problem setting.

In its Ising formulation, each vertex of the problem graph is represented by a spin. Each basis state then represents a set of vertices with spin up denoting a vertex that is in the set and spin down denoting a vertex that is not. For instance, the problem state $|E_a\rangle = |\downarrow\uparrow\uparrow\downarrow\uparrow\rangle$ corresponds to the set of vertices $\{2, 3, 5\}$. Note that this encoding results in the flipping of a spin corresponding to either adding or removing a vertex from the set. The vertex weights are implemented with local Z-fields and the independent set condition by introducing an edge penalty. This penalty is achieved by adding an antiferromagnetic ZZ-coupling, with a strength J_{zz} , between any two qubits corresponding to vertices connected by an edge. Assuming a high enough J_{zz} is chosen, the energies of the problem states will form clusters based on how many edges are contained in the corresponding set of vertices. The higher the magnitude of J_{zz} , the greater the separation between these clusters. Within the clusters, the energies of the states will be ordered by the total weight of the corresponding set, with the highest weighted set having the lowest energy.

A diagram of the scalable MWIS problem used in this work is shown in Fig. 2(a). It is a complete bipartite graph with n_0 vertices in sub-graph G_0 and n_1 vertices in sub-graph G_1 . As a result, the graph has two maximally independent sets giving the MWIS problem on this graph two local optima. We allocate a weight to each sub-graph, W_0 and W_1 , which we split equally between the vertices. We give each sub-graph a base weight of W and then increase the weight on sub-graph G_0 by δW such that $W_0 = W_1 + \delta W$ and $W_1 = W$. So long as δ is chosen to be small enough, this results in the set containing all the vertices in G_0 being the highest weighted

independent set and the set containing all the vertices in G_1 being the independent set with the second highest weight. An example graph with $n_0 = 2$ and $n_1 = 3$ is shown in Fig. 2(b).

The relative sizes of the sub-graphs dictate the energy spectra of the neighbourhoods around $|E_0\rangle$ and $|E_1\rangle$. Recall that flipping one of the spins in $|E_a\rangle$ from down to up corresponds to adding a vertex to the corresponding set and that flipping a spin from up to down corresponds to removing a vertex. This means that the neighbourhood around $|E_0\rangle$ has n_0 neighbours corresponding to independent sets and n_1 neighbours corresponding to dependent sets - and vice versa for $|E_1\rangle$. Recalling further that the states corresponding to independent sets have lower energies than those corresponding to dependent sets, we can say that if $n_1 > n_0$ then $|E_1\rangle$ has more low energy neighbours than $|E_0\rangle$.

Given a particular problem graph, we can use δW and $J_{\rm zz}$ to tune ΔE_{01} and the differences between the energies of the neighbourhoods around $|E_0\rangle$ and $|E_1\rangle$. Roughly speaking, we use δW to adjust ΔE_{01} and the edge penalty, J_{zz} , to change the separation between the clusters of problem energies associated with different numbers of edge violations. In practice however, the way in which we normalise H_p to keep the energy scale consistent means that both parameters have some effect on all the energy gaps in the spectrum. We are interested in how the effect of an XX-catalyst changes depending on the strength of the AC and so we choose our values of δW and J_{zz} to adjust the extent to which the problem state vectors are perturbed before the crossing while keeping the value of s for which the AC occurs for the 5-vertex instance (on which we focus our discussion) unchanged. Further details on our Hamiltonian and how we select our parameters can be found in appendix. A.

We now present numerical results corresponding to different parameter settings to confirm that we produce the desired AC and that we are able to alter its properties in the way described above. The results that we plot are the energy gaps between the instantaneous ground and first excited state, $\Delta E_{01}(s)$, as well as the evolution of the instantaneous ground state, $|E_0(s)\rangle$. The evolution of $|E_0(s)\rangle$ we consider in terms of the it's overlaps with the problem states - in particular with $|E_0\rangle$ and $|E_1\rangle$ since it is between these two states that we expect a crossing. Our results are obtained by numerical diagonalisation of H(s) at different values of s.

We first establish the presence of our AC. The left hand plot in Fig. 3(b) shows the gap spectrum for an anneal to a MWIS problem with $n_0=2,\ n_1=3,\ \delta W=0.01$ and $J_{\rm zz}=5.33$ in which we observe a gap minimum at s=0.9. The right hand plot shows the evolution of $|E_0(s)\rangle$ for the same graph and we see that the instantaneous ground state evolves towards $|E_1\rangle$ before there is a sharp exchange at s=0.9, where $|E_0(s)\rangle$ becomes dominated by $|E_0\rangle$. This transition along with the corresponding gap minimum is what we expect to see at the

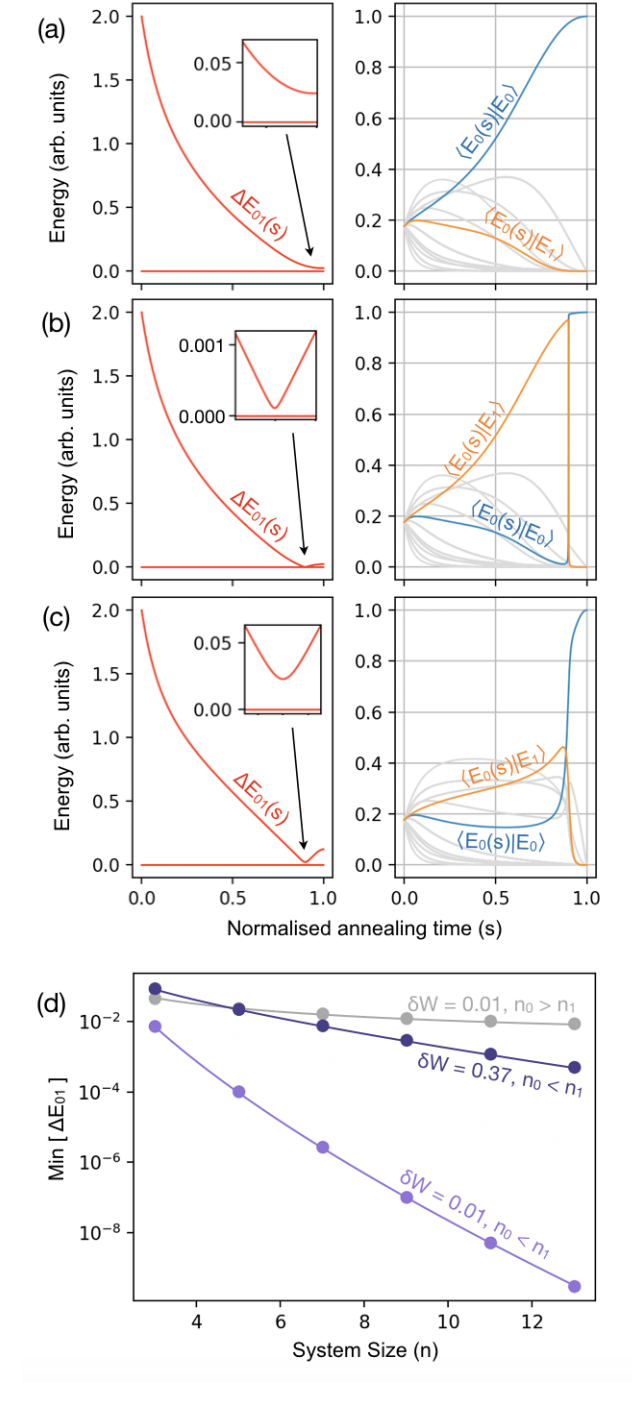


FIG. 3: (a-c) show numerical results for different anneals without the presence of a catalyst. Gap spectra are shown on the left and the evolution of the instantaneous ground state vector is shown on the right in terms of its overlaps with the problem states - the problem ground and first excited state overlaps are highlighted in blue and orange respectively. The problem parameters are: (a) $n_0 = 3$, $n_1 = 2$, $\delta W = 0.01$, $J_{zz} = 5.33$. (b) $n_0 = 2$, $n_1 = 3$, $\delta W = 0.01$, $J_{zz} = 5.33$ and (c) $n_0 = 2$, $n_1 = 3$, $\delta W = 0.37$, $J_{\rm zz}=37.5.$ (d) shows the minimum gap with increasing system size for three different parameter settings. The grey line corresponds to the parameter settings in (a) and the two purple lines correspond to the parameter settings in (b) and (c). The sub-graph sizes are scaled as $n_0 = (n-1)/2$ and $n_1 = (n+1)/2$. Lines in (d) connecting the data points are a guide to the eye.

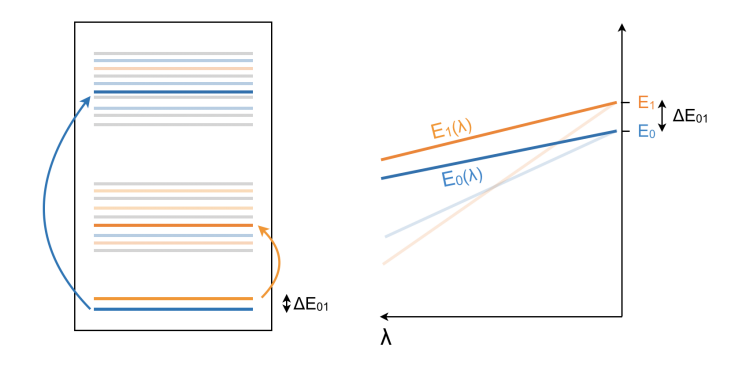


FIG. 4: Cartoon problem energy spectrum (left) and perturbed problem energies (right) corresponding to the same setting as Fig. 1(b) but with the addition of a catalyst. Left: Ground and first excited state, as well as their neighbourhoods, highlighted in blue and orange respectively. The neighbourhoods with respect to the driver Hamiltonian are shown in faded colours and the saturated lines with arrows to them show hypothetical new couplings from a catalyst. Right: The faded lines show the perturbed energies prior to the introduction of the catalyst and the saturated lines show the perturbed energies after the catalyst has been introduced - removing the crossing.

perturbative crossing. Finally, in Fig. 3(d), we present results for the scaling of the gap minimum with system size where we scale our sub-graph sizes as $n_0 = (n-1)/2$ and $n_1 = (n+1)/2$ and we use the same δW and J_{zz} as for our 5 vertex example. These results are plotted in the lighter purple and we see that the gap does indeed close exponentially. For comparison we also show, in Fig. 3, results for an anneal to a problem instance with the same parameters but the sub-graph sizes reversed so that there is no AC. Looking at Fig. 3(a) we see that no gap minimum forms towards the end of the anneal and the instantaneous ground state evolves smoothly towards the problem ground state. The scaling of the minimum gap with system size for this setting is plotted in grev in Fig. 3(d). We see that the gap size in this case does not close exponentially.

We now show how we can change our problem parameters to manipulate the AC in the desired way. In Fig. 3(c) we present results for the annealing gap spectrum and ground state evolution for a problem graph which again has $n_0 = 2$ and $n_1 = 3$ but where $\delta W = 0.37$ and $J_{\rm zz}=37.5$. That is, we have increased ΔE_{01} and enhanced the differences between the energies of the neighbourhoods around $|E_0\rangle$ and $|E_1\rangle$ such that the perturbed vectors undergo greater evolution before the perturbative crossing. Looking at the ground state evolution we see that by tuning the parameters in this way we are indeed able to adjust the extent to which the instantaneous ground state is dominated by $|E_1\rangle$ prior to the AC. We also see that, as expected, the gap minimum at the AC is larger than for the case depicted in 3(b) while it's location remains the same. Results for the gap scaling

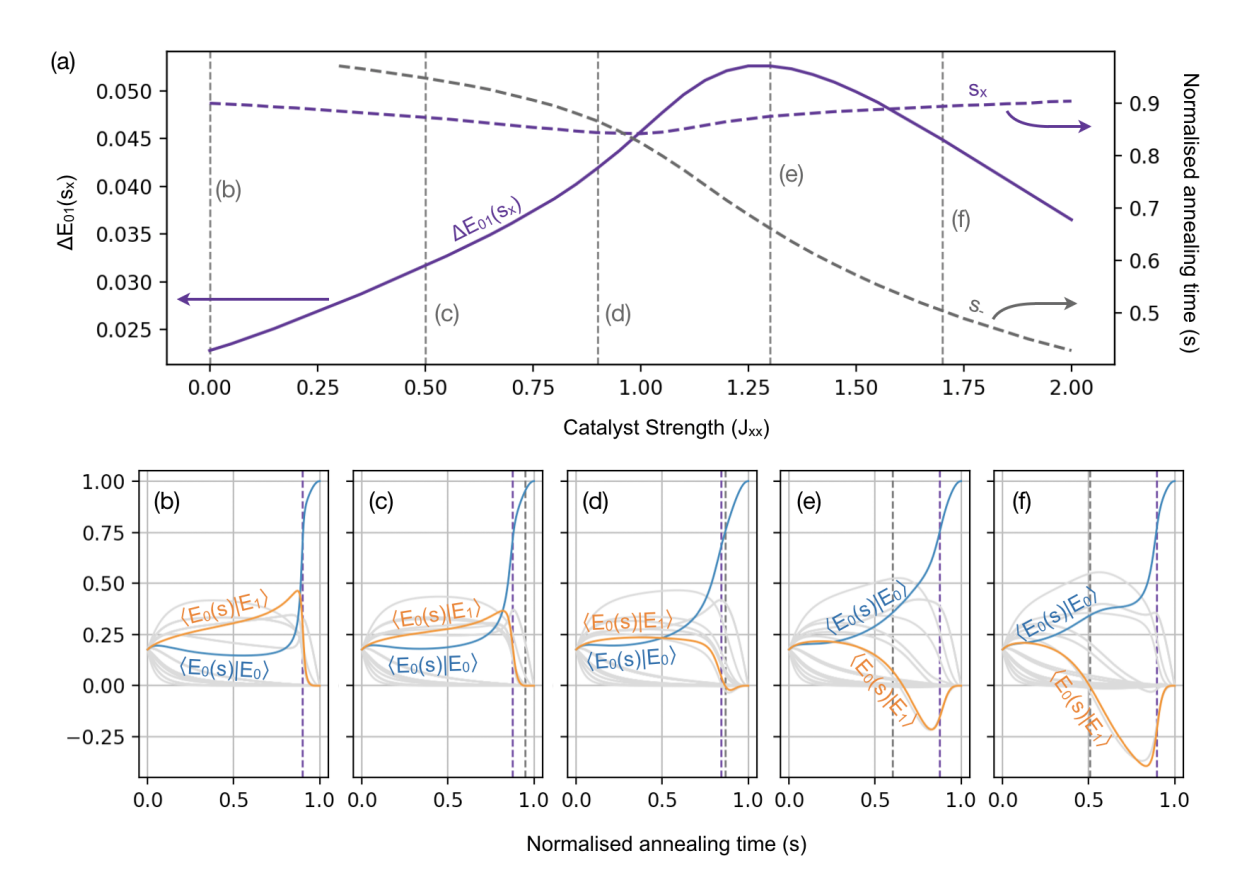


FIG. 5: Numerical results for a problem instance with $n_0=2$, $n_1=3$, $\delta W=0.37$ and $J_{zz}=37.5$. A catalyst is applied between a single pair of vertices in sub-graph G_1 . (a) shows the dependence on catalyst strength of the gap size at the AC, $\Delta E_{01}(s_{\rm x})$ (solid purple), the location of the minimum gap, $s_{\rm x}$ (dashed purple), and the value of s for which $\langle E_0(s)|E_1\rangle$ becomes negative, s_- (dashed grey). The evolution of the instantaneous ground state for different catalyst strengths is shown in (b-f). These plots have $s_{\rm x}$ and s_- marked with purple and grey dashed lines respectively. The catalyst strengths for which we show the evolution are marked on (a) with vertical grey dashed lines.

with system size corresponding to this new parameter setting is shown in Fig. 3(d) in dark purple. While the gap does still appear to close exponentially, we see that the exponent in this case is significantly milder. In the following, we will refer to our two problem parameter settings (which produce an AC) as the softer and harsher gap scaling cases.

III. XX-CATALYSTS

With our problem setting established, we now turn to the effects of introducing an XX-catalyst into the annealing Hamiltonian. As stated in section II A, the catalysts used in this work contain a single XX-coupling which is introduced into H(s) with the opposite sign to the driver and a strength of $|J_{xx}|$ (Eq. 5). This results in a non-stoquastic H(s) for $s \neq 0,1$ and as such it is possible for components of the instantaneous GS vector to become negative during the anneal. The XX-coupling we use is between a single pair of vertices in G_1 . (Symmetry in the problem means that there is no need to specify which two

are selected.) The result of this XX term is to couple $|E_1\rangle$ to a state corresponding to an independent set and $|E_0\rangle$ to a state corresponding to a dependent set - that is, the catalyst couples $|E_1\rangle$ to a state with significantly lower energy than it couples $|E_0\rangle$ to.

This choice of coupling is motivated by previous works [24, 25, 31] in which similar catalysts were shown to be able to soften or remove a perturbative crossing. One way in which this can been understood is by considering the additional energy corrections to E_0 and E_1 from introducing H_c as a perturbation to H_p . As with H_d , terms resulting from couplings to states with lower energies will result in larger corrections. However, the XX-coupling enters with the opposite sign to the driver and so its effect is to increase the energy of the problem states such that a larger correction to E_1 will result in a lifting of the crossing. We illustrate this effect in Fig. 4 which shows cartoons corresponding to the same setting depicted in Fig. 1(b) but with the addition of a catalyst.

In the following, we apply the catalyst to our scalable graph with the different parameter settings outlined in the previous section and compare the response of the gap spectra. We begin, in section III A, by applying our catalyst to the softer scaling case and find that, in this setting, the catalyst is able to enhance the minimum gap size and soften the gap scaling with system size. We discuss how the evolution of $|E_0(s)\rangle$ changes with increasing $J_{\rm xx}$ and how this corresponds to the changes to the gap spectrum - this will help set the stage for the following discussion and allow for comparison between the two cases. We then apply the same catalysts to the harsher gap scaling setting where the results are very different. While we do still see some gap enhancement in this setting, the scaling exponent appears unchanged. We also, for each system size, observe the closing of the gaps at the AC for particular catalyst strengths as well as the formation and closing of an additional gap minimum in the spectrum. We examine how the evolution of $|E_0(s)\rangle$ changes with J_{xx} and find that these closing gaps occur when the value of s at which we see sign changes in the instantaneous ground state vector components coincides with the location of a gap minimum in the spectrum.

A. Softer Scaling Setting

Numerical results corresponding to a graph with $n_0 =$ $2, n_1 = 3, \delta W = 0.37$ and $J_{zz} = 37.5$ are shown in Fig. 5. In the catalyst free case, these parameter choices result in the comparatively soft AC shown in Fig 3(c). The size of the gap minimum at the AC, $\Delta E_{01}(s_x)$, for varying J_{xx} is shown in Fig. 5(a) with a solid purple line. We observe that the introduction of the catalyst results in an enhancement to $\Delta E_{01}(s_x)$ up to an optimal catalyst strength of $J_{xx} = 1.30$ before the gap begins to close again. This existence of an optimal J_{xx} , rather than a monotonic improvement, was also observed in [24, 25]. Fig. 6(a) compares the gap scaling without the catalyst (black) and the gap scaling when we use a catalyst with $J_{\rm xx}$ optimised for each system size (purple) - the inset shows the optimal values of J_{xx} for each system size. We see that by using the optimal values we are able to greatly reduce the severity of the gap scaling with the optimised scaling appearing to be sub-exponential - although for these system sizes it is difficult to discern what the true scaling behaviour is.

Looking at the evolution of the ground state vector for $J_{xx}=0.0$, 0.5 and 0.9, shown in Figs. 5(b-d), we see a smoothing out of the changes in the problem state overlaps over the course of the anneal. We then see a resharpening of the exchange for $J_{xx}=1.3$ and 1.7, shown in Figs. 5(e-f), but with the overlap $\langle E_0(s)|E_1\rangle$ being negative. That the rate of change of the instantaneous ground state and the gap separating it from $|E_1(s)\rangle$ are related is well understood and expressions explicitly linking them can be found in [34]. The gradual smoothing out of the change in $|E_0(s)\rangle$ at the AC with the introduction of the catalyst is in line with the perturbative argument for the removal of the AC. As J_{xx} is increased, the value of the perturbative parameter, λ , for which

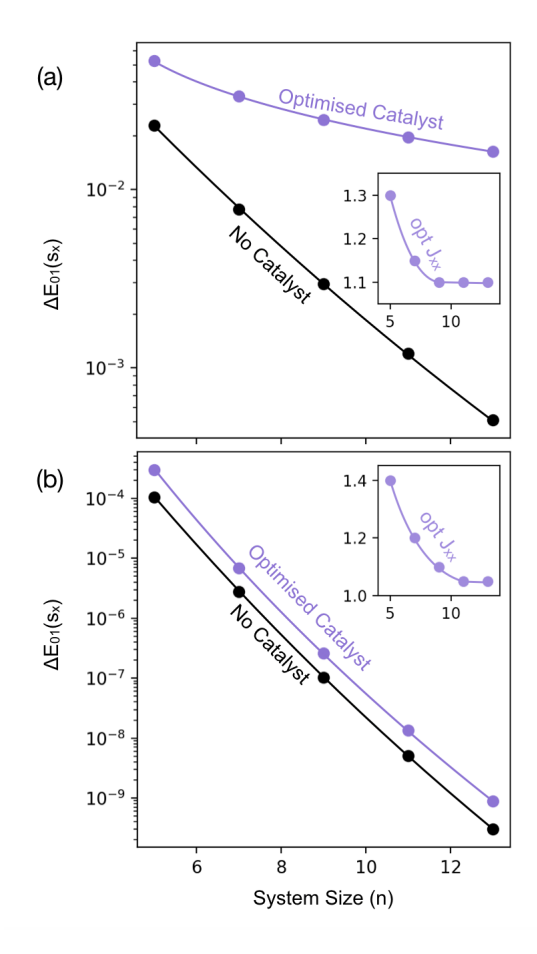


FIG. 6: Results for the size of the gap minimum at the AC with increasing system size. The sub-graph sizes are scaled as $n_0 = (n-1)/2$ and $n_1 = (n+1)/2$. (a) shows results for $\delta W = 0.37$ and $J_{zz} = 37.5$ and (b) shows results for $\delta W = 0.01$ and $J_{zz} = 5.33$. In each case we show the gap size without a catalyst in black and with J_{xx} chosen to maximise the gap size in purple. The values of J_{xx} that maximise the gap for each n are plotted in the insets. Lines connecting the data points are a guide to the eye.

 $E_0(\lambda)$ and $E_1(\lambda)$ intersect will increase. This will correspond to a decrease in the value of s at which we expect the AC to occur and an increase in the evolution of the perturbed problem state vectors away from $|E_0\rangle$ and $|E_1\rangle$ at the crossing point.

B. Harsher Scaling Setting

We now examine the effect of this same catalyst in harsher gap scaling setting. Numerical results for the size of the gap minimum at the AC for the 5-vertex instance at different catalyst strengths are presented in Fig. 7(a). We see that, as for the softer AC, the gap size does reach a maximum for an optimum catalyst strength. However, we also observe a closing of gap for $J_{xx} \approx 0.3$. Rather than the gap size reaching a well defined minimum, we

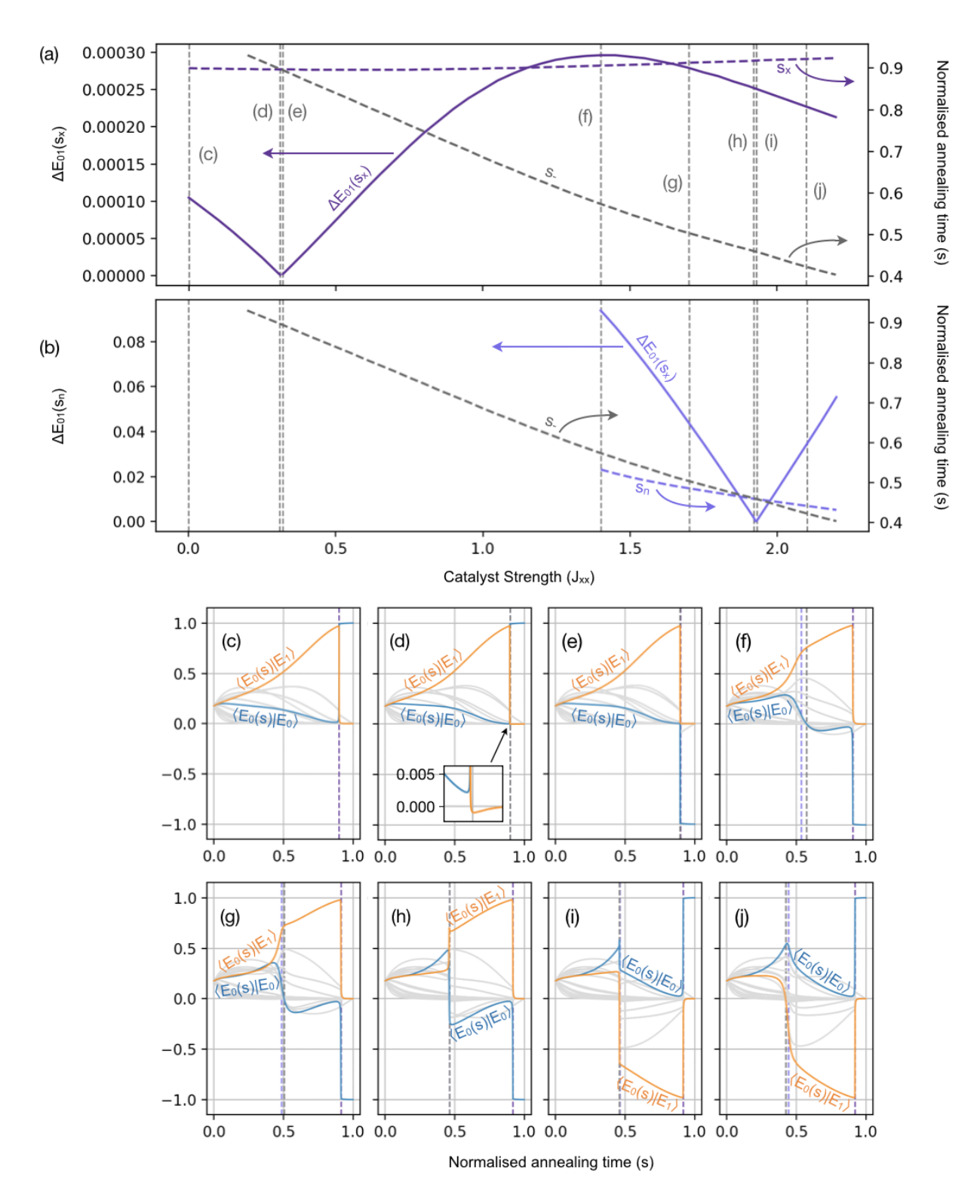


FIG. 7: Numerical results for a problem instance with $n_0 = 2$, $n_1 = 3$, $\delta W = 0.37$ and $J_{zz} = 37.5$. A catalyst is applied between a single pair of vertices in sub-graph G_1 . (a) shows, for increasing catalyst strength, results for the gap size at the AC, $\Delta E_{01}(s_x)$ (solid purple), the location of the minimum gap, s_x (dashed purple), and the value of s for which there is a sign change in either $\langle E_0(s)|E_0\rangle$ or $\langle E_0(s)|E_1\rangle$, s_- (dashed grey). (b) shows, for the same J_{xx} values, the gap size of the additional minimum gap that forms, $\Delta E_{01}(s_n)$ (solid lighter purple), the location of this additional minimum, s_n (dashed lighter purple) as well as s_- (dashed grey). Evolution of the instantaneous ground state for different catalyst strengths are shown in (c-j). These plots have s_x , s_n and s_- marked with the deeper purple, the lighter purple and grey respectively. The catalyst strengths for which we show the evolution are marked on (a) and (b) with vertical grey dashed lines.

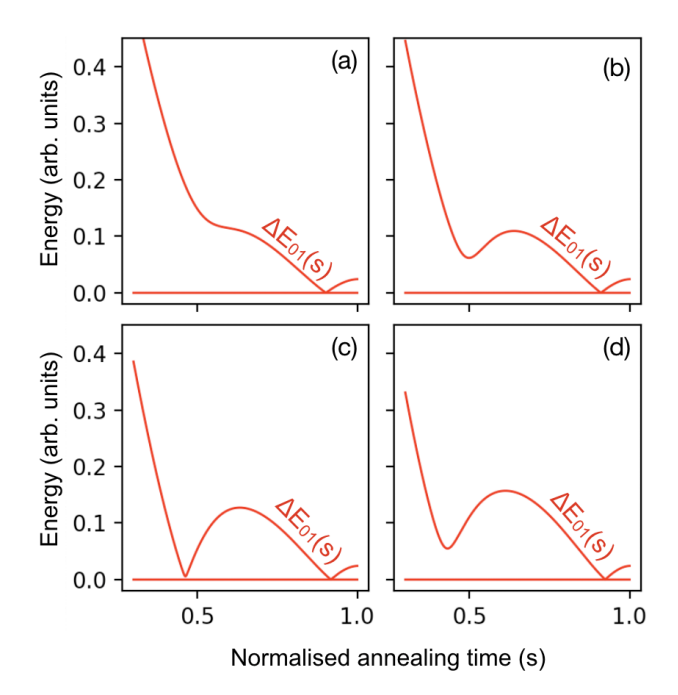


FIG. 8: Gap spectra for four different catalyst strengths showing the formation of an additional gap minimum between the instantaneous ground and first excited state. The problem parameters are $n_0 = 2$ $n_1 = 3$, $\delta W = 0.01$ and $J_{\rm zz} = 5.33$ and the catalyst is applied between two vertices in sub-graph G_1 . The catalyst strengths are $J_{\rm xx} = (a)$ 1.3 (b) 1.6 (c) 1.9 (d) 2.2

find that we are able to bring the gap size increasingly close to zero by increasingly fine tuning of J_{xx} . In addition to this we also observe the formation of a new gap minimum earlier in the spectrum - gap spectra showing this are presented in Fig. 8. We present the results for the gap size of this new minimum with increasing J_{xx} in Fig. 7(b). As with the gap minimum at the AC, we appear to be able to bring this gap size increasingly close to zero. Note that the plots in Figs. 7(a-b) correspond to exactly the same setting and that our separating the results for the two gap minima into different plots is only for readability of the data.

Another difference in the response of the gap spectra with these parameter settings is that, while we do still observe some gap enhancement at the AC, the catalyst does not significantly alter its scaling with the system size. We present in Fig. 6(b) results for the scaling of the gap minimum at the AC with and without the catalyst in purple and black respectively. As in the soft AC case, the J_{xx} used for each n is chosen to maximise the gap enhancement - these values are plotted in the inset. We observe that, while the gap size is increased for each n, the scaling exponent appears unchanged.

We now consider how the evolution of the ground state vector changes with increasing J_{xx} in order to shed some light on the closing gaps that we observe - beginning with a discussion on the relative signs between the vector com-

ponents of the instantaneous ground state as a result of the introduction of our catalyst. As noted previously, the non-stoquastic nature of our Hamiltonian means we can expect some of the vector components to become negative at some point over the course of the anneal. We can also expect the couplings present in the catalyst to influence the relative signs between the vector components [25]. Looking at Figs 5(b-f) and 7(c-j) we see that, for our problem setting and choice of catalyst, the components corresponding to the problem ground and first excited states take opposite signs at some s given sufficiently large J_{xx} - we refer to this value of s as s_- . We also see that as we increase J_{xx} , the value of s_{-} decreases. This can be understood by the fact that this change in signs is associated with the non-stoquasticity introduced by the catalyst and that a greater J_{xx} will result in the catalyst reaching greater relative strengths in comparison to the driver earlier in the anneal.

We now return to Fig. 7(a). In addition to the size of the gap minimum associated with the AC, we show the location of this gap minimum, s_x with a dashed purple line, and s_{-} with a dashed grey line. We see that the closing gap is observed for the J_{xx} value at which $s_{-} = s_{x}$. Fig. 7(b) shows the same data but for the additional gap minimum that forms in the harsher AC setting - in this case we denote the location of this minimum with s_n . We see again that this new gap minimum approaches zero for the J_{xx} value at which $s_{-}=s_{\rm n}$. Associating the closing gaps with values of J_{xx} at which the minimum gap locations coincide with with s_{-} is however not sufficient to account for the differing behaviours in the softer and harsher scaling settings. Looking at Fig. 5(a) from the preceding section, we see that there is also a value of J_{xx} for which $s_{-} = s_{x}$ however no closing of the gap at the AC is observed.

To better understand the differences in the behaviour in these two regimes we compare how the evolution of the ground state vector changes with J_{xx} . We plot the evolution of the ground state vector in the harsher scaling case at different J_{xx} values in Figs. 7(c-j). In each plot, $s_{\rm x}$, $s_{\rm n}$ and $s_{\rm -}$ are marked in dark purple, light purple and grey respectively and the J_{xx} values to which these plots correspond are marked in Figs. 7(a-b) with vertical dashed grey lines. Looking at the plots corresponding to $J_{xx} = 0$ and 0.31, Figs. 7(c) and (d), we see that as we increase J_{xx} towards the value at which $E_{01}(s_x)$ vanishes, there is a sharpening of the change in the vector components around s_x . Then, as s_- passes s_x , which happens between Figs. 7(d) and (e), there appears to be a discontinuous change in which overlap crosses zero. After this point, the change in $|E_0(s)\rangle$ around s_x begins to soften again. Looking at the Figs. 7(f-j), we see the same sharpening (up to $J_{xx} = 1.92$ in Fig. 7(h)) and then softening of the rate of change in $|E_0(s)\rangle$ around the location of the additional gap minimum, s_n . We also observe another shift in which vector component crosses zero as s_{-} passes s_{n} - which occurs between Figs. 7(h-i).

This behaviour is in stark contrast to the softer scal-

ing case where no distinct changes are observed around the J_{xx} value where $s_{-} = s_{x}$. It is unclear why exactly this should be the case however we can comment on some differences we observe between the two settings. In the case where the original AC is softer, the AC has already become significantly smoothed out for the the J_{xx} where $s_{-}=s_{x}$. This is in contrast to the hard AC setting where the magnitudes of $|\langle E_0(s)|E_0\rangle|$ and $|\langle E_0(s)|E_1\rangle|$ that are exchanged at the AC is largely unchanged for the J_{xx} value at which $s_{-} = s_{x}$. This is at least partially explained by the fact that if the initial AC is softer, we can expect that a smaller change to the Hamiltonian is required to lift it. We also note that s_{-} does not appear until higher values of J_{xx} in the softer scaling setting and the catalyst strength for which s_{-} passes s_{x} is over three times as high as it is for the harsher scaling case such that it may be possible to lift the AC to a greater extent before reaching the J_{xx} for which $s_{-} = s_{x}$.

We now present data examining intermediate parameter settings to further understand the changing behaviour as we move from the harsher to the softer gap scaling case. In Fig. 9 we plot the J_{xx} values associated with the two closing gaps for the 5-vertex instance with seven different parameter settings. The x-axis gives the δW used for each parameter setting however we note the the edge penalty, J_{zz} , is also changing between each data point - with its value in each case chosen such that $s_{\rm x}=0.9$ without the presence of a catalyst. We observe that the two J_{xx} values approach each other as we adjust the parameters to soften the AC present in the original annealing spectrum until both values disappear at $\delta W \approx 0.13$. Given that the closing gaps are associated with a change in which vector component changes sign, one interpretation of these results could be that the lack of closing gaps in the softer AC setting is due to the vanishing of the J_{xx} range for which the vector component corresponding to the problem ground state crosses zero.

So far we have only considered the effect of the catalyst on annealing spectra corresponding to our very simple MWIS graph shown in Fig. 2. This was so we could examine the differing effects from the catalyst in the most straightforward setting. However, we note that we observe these closing gaps for more general MWIS instances with additional local optima such that the problem Hamiltonian has more excited states with energy comparable to that of the ground state. These instances can be constructed in much the same way as the problem graph shown in Fig. 2(a). but with additional sub-graphs such that we have a complete k-partite graph. Further detail found on the construction of these more general instances can be found in appendix B. The catalysts were applied to instances with up to four sub-graphs and in each case the coupling was chosen to be within the subgraph corresponding to the excited problem state associated with the AC involving the ground state. For all the examples examined, we observed a closing of the gap at the AC as well as the the formation of an additional

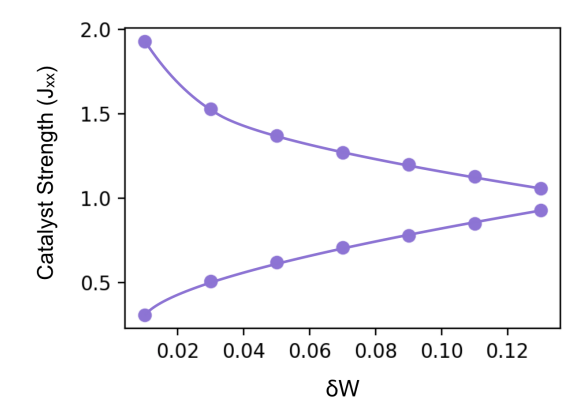


FIG. 9: J_{xx} values at which the gaps go to zero for different parameter settings. The x-axis shows the δW values for each parameter setting. The corresponding J_{zz} value for each case is chosen such that $s_x = 0.9$. Lines connecting the data points are a guide to the eye.

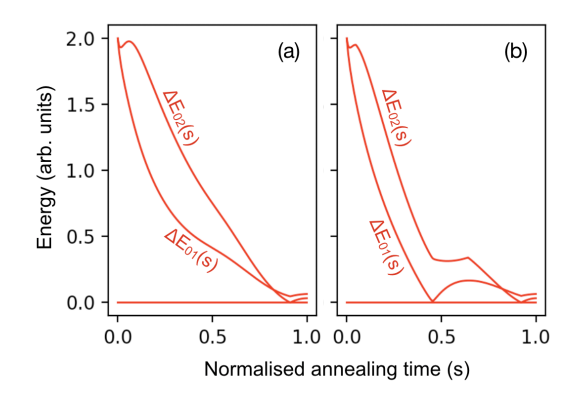


FIG. 10: Gap spectra for an anneal corresponding to a MWIS problem with two local optima in addition to the global optimum. The results with and without a catalyst are shown in (b) and (a) respectively. Details on the construction of this problem instance and the catalyst used are given in appendix B.

gap minimum between the instantaneous ground and first excited states - suggesting that the effects from the catalyst described in this section may be a more general phenomenon.

IV. DISCUSSION

We have examined the effects of specific XX-catalysts on annealing spectra corresponding to small instances of the MWIS problem. In particular, we have examined how the effect of a targeted XX-coupling, chosen to enhance the gap size at a perturbative crossing, differs depending on the nature of the AC that is present in the spectrum. We found that the response of the gap spectra to the introduction of the catalyst was highly sensitive to subtle changes in the encoding of the problem which affected the

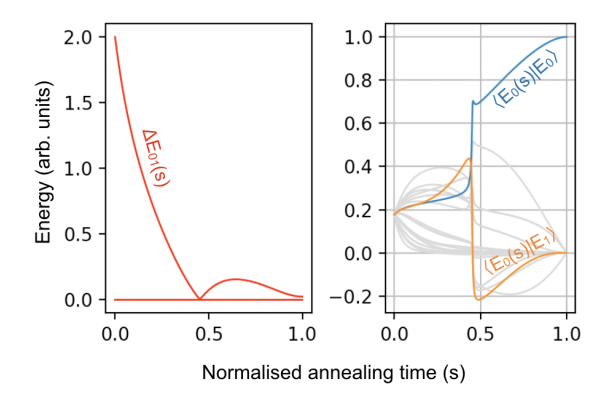


FIG. 11: Gap spectrum and ground state evolution for a problem instance with $n_0 = 3$, $n_1 = 2$, $\delta W = 0.01$ and $J_{zz} = 5.33$ and a catalyst containing one coupling within G_0 . (Results for this problem instance without a catalyst can be found in Fig. 3(a).)

scaling of the gap at the AC with system size.

More specifically, we found that for parameter settings that resulted in a softer AC, the catalyst resulted in an enhancement of the gap minimum, and that if an optimised catalyst strength was used for each system size, the gap scaling could be significantly improved. We then applied the same catalysts to the case where we chose our problem parameters to produce an AC with harsher gap scaling and found that, while some gap enhancement was possible, the catalyst was not able to provide the same improvement in scaling. In addition, we found that in this setting the catalyst could result in the closing of the gap at the AC, as well as the production of an additional gap minimum in the spectrum, if introduced with particular magnitudes. These results suggest that the catalysts we examine here may be less successful in suppressing the gap scaling at an AC when the original gap scaling is less favourable. More generally, they show that small changes to the problem parameters can result in the same catalyst having strikingly different effects meaning that great care may be required when designing a catalyst.

In order to understand the closing gaps in the harsher gap scaling setting, we examined the evolution of the instantaneous ground state at varying catalyst strengths. Gap closing occurred when the value of s for which we saw sign changes in the ground state vector components coincided with the location of a gap minimum. While catalyst strengths for which these values coincided were found to exist in both the settings examined in this work, we observed that in the harsher AC setting, this was accompanied by a increase in the rate of change of the ground state vector around the location of the gap minimum as well as a change in which vector components became negative. We suggested that the difference in behaviour between the two settings may relate to the extent that the perturbative crossing has been lifted for the catalyst strength at which the two s values coincided.

Interestingly, while the targeted catalyst did not re-

sult in the intended suppression to the gap scaling in the harsher AC setting, the resultant spectrum does appear amenable to a diabatic anneal. That is, rather than running the algorithm slowly enough that the system remains in the ground state, the system could be allowed to transition into the first excited state at the first small gap (the new gap minimum produced by the catalyst) and then back into the ground state at the second (the gap minimum corresponding to the AC present in the original annealing spectrum). Initial dynamic simulations for the 5-qubit case suggest that this is indeed possible and results in a significant reduction to the annealing time required for the system to end the anneal in the problem ground state. These results are presented in appendix C.

However, the setting examined in this work is very specific as it has been constructed solely to allow for the production and tuning of a single perturbative crossing - rather than to create a realistic problem setting. If we consider the effect of this catalyst on annealing spectra corresponding to even slightly more general MWIS problems, we see that the production of the additional gap minimum cannot generally be expected to result in a setting suitable to DQA. For instance, consider the example energy spectra presented in Fig. 10 where we have introduced an additional local optimum. Here, the additional gap minimum results in a setting where the system is likely to evolve to the second excited state if the anneal is run diabatically. We note that if the anneal is run without a catalyst, the energy spectrum suggests that the system is likely to evolve to the first excited state meaning that, in this case, the additional gap minimum not only fails to help the system reach the ground state, but it actually reduces the quality of the solution found. We therefore suggest that, while the mechanism responsible for this additional gap minimum may be of interest for manipulating the gap spectrum, the changes to the gap spectrum we observe in this work are not in general useful for creating a gap spectrum suitable to DQA.

We note that the formation of the additional gap minimum that we observe in the harsher scaling case is not intrinsically linked to the presence of a perturbative crossing in the original annealing spectrum. We demonstrate this in Fig. 11 which shows results for the gap spectrum and ground state evolution when a catalyst is applied to the setting without an AC shown in Fig. 3(a). The catalyst contains an XX-coupling within G_0 such it couples $|E_0\rangle$ to a lower energy state than it couples $|E_1\rangle$ to. We suggest that the formation of the new gap minimum may relate to the existence of a $J_{\rm xx}$ value for which both the problem ground and first excited state components of the instantaneous ground state vector have appreciable magnitudes in the vicinity of s_- such that either component crossing zero results in a sharp change in the coefficients.

We argue that the reason such a value is observed for the setting without an AC as well as the harsher AC setting (but not for the softer AC) relates to the magnitudes of key ground state vector components in the original annealing spectrum. Effectively, what we are doing with the introduction of our catalyst is to guide the anneal away from a particular problem state, which has the effect of suppressing the magnitude of the corresponding vector component in the instantaneous ground state. For the two settings with perturbative crossings that we examined this is the component corresponding to the problem first excited state and for the setting without a perturbative crossing this is the component corresponding to the problem ground state. What the setting without an AC and the harsher AC setting have in common is that the magnitude of this component approaches 1 in the original annealing spectrum without a catalyst - as can be seen in Figs. 3(a-b). Looking at Figs. 3(c), we see that in the softer AC setting, the maximum magnitude reached is only around 0.45. Thus, the problem state that our catalyst is guiding the anneal away from reaches greater levels of suppression for the same J_{xx} values in this setting than it does in the other two. This goes hand in hand with our earlier observation that, unlike in the harsh gap scaling setting, the AC is already significantly lifted in the soft AC setting for the J_{xx} value at which $s_x = s_-$.

It is not yet clear whether the behaviour we observe in these two settings will scale to larger system sizes. Regarding the gap enhancement in the softer AC setting, the optimal J_{xx} appears to quickly approach a constant see inset in Fig. 6(a). This is interesting as it implies that a single XX-coupling applied at a constant strength can be used to lift a perturbative crossing - even as this single coupling becomes negligible with respect to the system it is being applied to. While this seems counter-intuitive, such phenomena are not unfamiliar in physics, where a single impurity spin in a system can have a significant effect [35, 36]. That being said, the system sizes that we have looked at may not be sufficient to determine the true scaling behaviour. If the scaling trend does persist however, this would be very promising since the number of potential XX-couplings scales as the square of the system size. This means that if only one is required, an appropriate coupling may be able to be found in polynomial time using trial and error.

The way in which we scale our problem graph in this work is to increase the number of vertices while keeping the number of local optima the same. However, in a realistic setting, one would expect the number of local optima to scale with the problem size. For this reason it is important to study how the effect of the catalyst changes with the introduction of additional local optima. Potentially we might expect a situation analogous to that discussed in [37] where the strengths of the local transverse fields of the driver are adjusted recursively using information from repeated annealing runs in order to remove the different perturbative crossings that form. A similar procedure may be possible with the inclusion of a new XX-coupling at each iteration - chosen to couple the local optima that QA returns to low energy states.

It also remains to be seen whether or not there continues to exist a regime where we observe the closing gaps and where the catalyst does not reduce the gap scaling as we move to larger problems. Something to consider in this respect may be how the boundary between the two regimes changes with respect to different problem parameters as we increase the system size. With regards to the existence of additional local optima, we have observed the behaviour we associated with the harsher gap scaling for all the graphs examined in this work - however we have so far only looked at problems with up to 13 spins and 4 local optima. Further numerical investigation, and a better understanding of what causes the closing gaps that we have observed, are required to establish under what conditions we will observe the contrasting effects examined in this paper, and so how our findings may translate to more realistic problem settings.

ACKNOWLEDGMENTS

We gratefully acknowledge Vicky Choi, Daniel O'Connor and Robert Banks for inspiring discussion and helpful comments. This work is supported by EPSRC, grant references EP/S021582/1 and EP/T001062/1.

- [1] B. Apolloni and D. D. Falco, Quantum Stochastic Optimization, Stochastic Processes and their Applications **33**, 233 (1989).
- [2] A. B. Finnila, M. A. Gomez, C. Sebenik, C. Stenson, and J. D. Doll, Quantum annealing: A new method for minimizing multidimensional functions, Chemical Physics Letters 219, 343 (1994), arXiv:9404003 [chem-ph].
- [3] T. Kadowaki and H. Nishimori, Quantum annealing in the transverse Ising model, Phys. Rev. E 58, 5355 (1998), arXiv:9804280 [cond-mat].
- [4] Tosio Kato, On the Adiabatic Theorem of Quantum Mechanics, Journal of the Physical Society of Japan 5, 435 (1950).
- [5] E. Farhi, J. Goldstone, S. Gutmann, J. Lapan, A. Lundgren, and D. Preda, A quantum adiabatic evolution algorithm applied to random instances of an np-complete

- problem, Science 292, 472-475 (2001).
- [6] A. P. Young, S. Knysh, and V. N. Smelyanskiy, First-order phase transition in the quantum adiabatic algorithm, Physical Review Letters 104, 1 (2010), arXiv:0910.1378.
- [7] T. Jörg, F. Krzakala, J. Kurchan, and A. C. Maggs, Quantum annealing of hard problems, Progress of Theoretical Physics 184, 290 (2010), arXiv:0910.5644.
- [8] T. Jörg, F. Krzakala, J. Kurchan, A. C. Maggs, and J. Pujos, Energy gaps in quantum first-order meanfield-like transitions: The problems that quantum annealing cannot solve, EPL (Europhysics Letters) 89, 40004 (2010).
- [9] B. Seoane and H. Nishimori, Many-body transverse interactions in the quantum annealing of the p-spin ferromagnet, Journal of Physics A: Mathematical and Theoretical

- 45, 435301 (2012), arXiv:1207.2909.
- [10] S. Knysh, Zero-temperature quantum annealing bottlenecks in the spin-glass phase, Nature Communications 7, 12370 (2016).
- [11] M. H. Amin and V. Choi, First-order quantum phase transition in adiabatic quantum computation, Phys. Rev. A 80, 062326 (2009), arXiv:0904.1387.
- [12] B. Altshuler, H. Krovi, and J. Roland, Anderson localization makes adiabatic quantum optimization fail, Proceedings of the National Academy of Sciences 107, 12446 (2010).
- [13] E. Farhi, J. Goldstone, D. Gosset, S. Gutmann, H. B. Meyer, and P. Shor, Quantum adiabatic algorithms, small gaps, and different paths, Quantum Information and Computation 11, 181 (2011), arXiv:0909.4766.
- [14] N. G. Dickson and M. H. Amin, Does adiabatic quantum optimization fail for NP-complete problems?, Physical Review Letters 106, 050502 (2011), arXiv:1010.0669.
- [15] Y. Susa, Y. Yamashiro, M. Yamamoto, and H. Nishimori, Exponential speedup of quantum annealing by inhomogeneous driving of the transverse field, Journal of the Physical Society of Japan 87, 4 (2018), arXiv:1801.02005.
- [16] K. Takada, Y. Yamashiro, and H. Nishimori, Mean-field solution of the weak-strong cluster problem for quantum annealing with stoquastic and non-stoquastic catalysts, Journal of the Physical Society of Japan 89, 1 (2020), arXiv:1912.09189.
- [17] L. Fry-Bouriaux, D. T. O'Connor, N. Feinstein, and P. A. Warburton, Locally suppressed transverse-field protocol for diabatic quantum annealing, Phys. Rev. A 104, 435301 (2021).
- [18] J. I. Adame, P. L. McMahon, and P. L. McMahon, Inhomogeneous driving in quantum annealers can result in orders-of-magnitude improvements in performance, Quantum Science and Technology 5, 435301 (2020), arXiv:1806.11091.
- [19] M. M. Rams, M. Mohseni, and A. D. Campo, Inhomogeneous quasi-adiabatic driving of quantum critical dynamics in weakly disordered spin chains, New Journal of Physics 18, 123034 (2016), arXiv:1606.07740.
- [20] E. Farhi, J. Goldstone, and S. Gutmann, Quantum adiabatic evolution algorithms with different paths (2002), arXiv:quant-ph/0208135 [quant-ph].
- [21] Y. Seki and H. Nishimori, Quantum annealing with antiferromagnetic transverse interactions for the Hopfield model, Journal of Physics A: Mathematical and Theoretical 48, 335301 (2015), arXiv:1410.0450.
- [22] L. Hormozi, E. W. Brown, G. Carleo, and M. Troyer, Nonstoquastic Hamiltonians and quantum annealing of an Ising spin glass, Phys. Rev. B 95, 184416 (2017), arXiv:1609.06558.
- [23] H. Nishimori and K. Takada, Exponential enhancement of the efficiency of quantum annealing by non-stoquastic Hamiltonians, Frontiers in ICT 4, 10.3389/fict.2017.00002 (2017), arXiv:1609.03785.
- [24] T. Albash, Role of nonstoquastic catalysts in quantum adiabatic optimization, Phys. Rev. A 99, 042334 (2019), arXiv:1811.09980.
- [25] V. Choi, Essentiality of the Non-stoquastic Hamiltonians and Driver Graph Design in Quantum Optimization Annealing (2021), arXiv:2105.02110.
- [26] T. Albash and M. Kowalsky, Diagonal catalysts in quantum adiabatic optimization, Phys. Rev. A 103, 022608 (2021), arXiv:2009.05726.

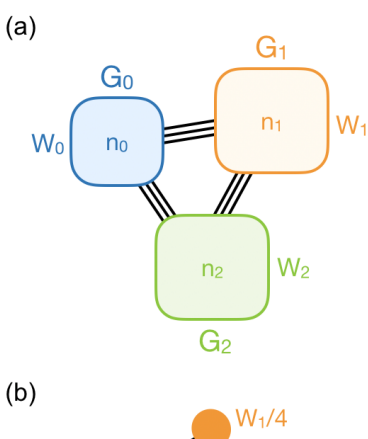
- [27] V. Mehta, F. Jin, H. De Raedt, and K. Michielsen, Quantum annealing with trigger hamiltonians: Application to 2-satisfiability and nonstoquastic problems, Phys. Rev. A 104, 032421 (2021).
- [28] R. D. Somma, D. Nagaj, and M. Kieferová, Quantum speedup by quantum annealing, Physical Review Letters 109, 050501 (2012).
- [29] K. Takada, S. Sota, S. Yunoki, B. Pokharel, H. Nishi-mori, and D. A. Lidar, Phase transitions in the frustrated ising ladder with stoquastic and nonstoquastic catalysts, Physical Review Research 3, 043013 (2021).
- [30] E. Crosson, T. Albash, I. Hen, and A. P. Young, Designing Hamiltonians for quantum adiabatic optimization, Quantum 4, 334 (2020), arXiv:2004.07681.
- [31] V. Choi, The effects of the problem Hamiltonian parameters on the minimum spectral gap in adiabatic quantum optimization, Quantum Information Processing 19, 90 (2020), arXiv:1910.02985.
- [32] L. Gupta and I. Hen, Elucidating the interplay between non-stoquasticity and the sign problem (2019), arXiv:1910.13867 [quant-ph].
- [33] M. H. Amin, Effect of local minima on adiabatic quantum optimization, Physical Review Letters 100, 130503 (2008), arXiv:0709.0528.
- [34] A. Braida and S. Martiel, Anti-crossings and spectral gap during quantum adiabatic evolution (2021), arXiv:2102.00987.
- [35] S. Eggert and I. Affleck, Magnetic impurities in halfinteger-spin heisenberg antiferromagnetic chains, Phys. Rev. B 46, 10866 (1992).
- [36] N. Laflorencie, E. S. Sørensen, and I. Affleck, The kondo effect in spin chains, Journal of Statistical Mechanics: Theory and Experiment 2008, P02007 (2008).
- [37] N. G. Dickson and M. H. Amin, Algorithmic approach to adiabatic quantum optimization, Phys. Rev. A 85, 1 (2012), arXiv:1108.3303.

Appendix A: MWIS Problem Parameters

Our MWIS problem Hamiltonian is given by

$$H_p = \sum_{i \in \{\text{vertices}\}} (c_i J_{zz} - 2w_i) \sigma_i^z + \sum_{(i,j) \in \{\text{edges}\}} J_{zz} \sigma_i^z \sigma_j^z \quad (A1)$$

where c_i is the number of edges connected to vertex i, w_i is the weight on vertex i, and $J_{\rm zz}$ is the edge penalty. As discussed in section IIB, our problem instances are on complete bipartite graphs and we label the two disconnected sub-graphs as G_0 and G_1 - as shown in Fig 2. We allocate a total weight of 1 to G_1 and a total weight of $1 + \delta W$ to G_0 . This weight is split evenly between the vertices in each sub-graph. To get a clearer picture of what parameters we can change to define our problem instances within this structure, we can re-write Eq. A1



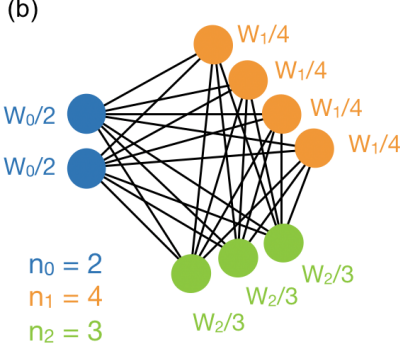


FIG. 12: An illustration of a tri-partite graph constructed as described in appendix B is shown in (a). An example with $n_0 = 2$, $n_1 = 4$ and $n_2 = 3$ is shown in (b). This is the example corresponding to the annealing spectra in Fig. 10.

as

$$H_{p} = (n_{1}J_{zz} - \frac{2(1 + \delta W)}{n_{0}}) \sum_{i \in G_{0}} \sigma_{i}^{z} + (n_{0}J_{zz} - \frac{2}{n_{1}}) \sum_{i \in G_{1}} \sigma_{i}^{z} + J_{zz} \sum_{i \in G_{0}} \sum_{j \in G_{1}} \sigma_{i}^{z} \sigma_{j}^{z},$$

where n_0 and n_1 are the number of vertices in G_0 and G_1 respectively. For a particular problem graph defined by n_0 and n_1 , the free parameters are then δW and J_{zz} .

So that we do not change the energy scale of the problem Hamiltonian when we adjust the values of δW and J_{zz} , we normalise the parameters that go into Eq. A1. For a set of parameter values $(\delta W, J'_{zz})$, we first calculate the un-normalised vertex weights as $w'_i = (1 + \delta W)/n_0$ for $i \in G_0$ and $w'_i = 1/n_1$ for $i \in G_1$, giving us our set of un-normalised parameters $(\{w'_i\}, J'_{zz})$. We then obtain our normalised parameters as

$$w_i = Kw_i', J_{zz} = KJ_{zz}'$$

where

$$K = \frac{E_{\text{scale}} \times n}{4(N_{\text{edges}} \times J'_{\text{zz}} - W)} = \frac{E_{\text{scale}} \times (n_0 + n_1)}{4(n_0 \times n_1 \times J'_{\text{zz}} - 1)}$$

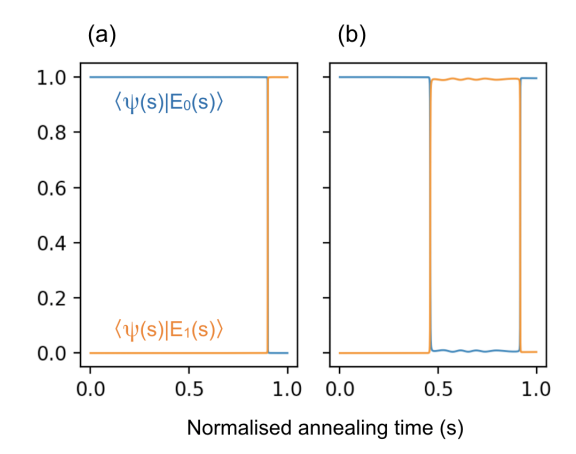


FIG. 13: Results showing the dynamics of an anneal on a problem graph with $n_0 = 2$, $n_1 = 3$, $\delta W = 0.01$ and $J_{\rm zz} = 5.33$ in a closed system setting. This evolution is presented in terms of the system's overlap with the instantaneous ground and first excited states in blue and orange respectively. The total annealing time used is $T_{\rm anneal} = 0.01$ in comparison to the local driver fields being introduced with a magnitude of 1. (a) shows the results without a catalyst and (b) shows the results using a catalyst with $J_{\rm xx} = 1.92$.

and E_{scale} sets the energy scale in relation to the driver.

We choose our problem parameters with reference to our five vertex instance $(n_0 = 2 \text{ and } n_1 = 3)$ since this is the instance for which we present data for the whole anneal rather than just e.g the minimum gap value. Our different parameter sets $(\delta W, J'_{zz})$ are chosen by first selecting our δW and then, through trial and error, adjusting our un-normalised J'_{zz} so that $s_x = 0.9$ in the annealing spectrum to corresponding to our normalised problem Hamiltonian for our 5-vertex example.

Appendix B: Introducing Additional Local Optima

We describe here how our problem graph can be generalised to include additional local optima. This can be done straightforwardly by adding further sub-graphs for each additional local optima to produce a complete kpartite graph. That is we have k sub-graphs where each vertex in every sub-graph is connected to every vertex in every other sub-graph and there are no connections within the sub-graphs themselves. Each local optimum then corresponds to picking all the vertices from one of the sub-graphs. As with our bipartite graphs, each subgraph G_a is given n_a vertices which decides the energy spectrum of neighbourhood of the corresponding problem state. It is also given a total weight, W_a , which is shared out equally between its vertices such that each vertex in G_a has a weight of W_a/n_a . A general tri-partite graph is shown in Fig. 12(a) and a specific example is shown in Fig. 12(b). However, more sub-graphs can be added.

Appendix C: Diabatic Anneal on the 5-vertex Graph

We present here numerical results for the dynamics of an anneal to our 5-vertex problem instance with the harsher gap scaling. These results are obtained using closed system spin models and the evolution of the system is presented in terms of its overlap with the instantaneous ground and first excited states. Since we have not specified a true energy scale we can cannot discuss the evolution with respect to an actual annealing time but only in relation to the magnitude we introduce our Hamiltonian with.

The annealing time used in these simulations was 0.1 in relation to the local driver fields being introduced with a magnitude of 1. Fig. 13(a) shows the evolution without a catalyst and we see that for this annealing time the system has a negligible overlap with the problem ground state at the end of the anneal - after transitioning into the first excited state at the avoided level crossing. Fig. 13(a) shows the results when our catalyst is introduced with $J_{xx}=1.92$, such that another small gap in the spectrum is produced. We observe that in this case the system ends the anneal with a near unity overlap with the problem ground state as a result of transitioning into the first excited state at the first small gap and then back into the ground state at the second.